PHILOSOPHICAL TRANSACTIONS OF THE ROYAL SOCIETY A MATHEMATICAL, PHYSICAL & ENGINEERING SCIENCES

On the Advection of Spherical and Non-Spherical Particles in a Non-Uniform Flow

M. R. Maxey

Phil. Trans. R. Soc. Lond. A 1990 **333**, 289-307
doi: 10.1098/rsta.1990.0162

On the advection of spherical and non-spherical particles in a non-uniform flow

By M. R. Maxey

Center for Fluid Mechanics, Turbulence and Computation, Brown University, Providence, Rhode Island 02912, U.S.A.

Small spherical particles when introduced into a non-uniform or unsteady flow are usually subject to inertial effects, either of the particle mass or of the fluid added-mass, and the gravitational settling. Small non-spherical particles, even when inertial effects are negligible, turn in response to the local fluid velocity gradients and the settling velocity of a particle varies with its orientation. These features are distinct from the response of lagrangian elements which simply move with the local fluid velocity. In this paper these different responses for small, stokesian particles are considered for some example non-uniform laminar flows. It is noted that this added feature may lead to chaotic particle motion where the motion of lagrangian elements is regular, and conversely regular motion where there is chaotic advection of lagrangian elements.

1. Introduction

The study of the lagrangian motion of fluid elements has long been a focus of work on mixing processes. The mean concentration of a passive scalar contaminant subject to random stirring may effectively be estimated from the lagrangian statistics of fluid motion. This is exemplified by the paper of Taylor (1921) who showed how an effective turbulent dispersion coefficient would result from the action of stationary, homogeneous turbulence on fluid elements. These ideas were developed further by Batchelor (1949), Batchelor & Townsend (1956) and Corrsin (1952) among others. The underlying principle is that turbulent mixing is a much more effective process than molecular diffusion for a scalar contaminant and that in determining at least the mean concentration molecular diffusion may be ignored. Under this assumption the local concentration $c(\boldsymbol{x}, t)$ in an incompressible flow $\boldsymbol{u}(\boldsymbol{x}, t)$ is determined solely by the advection of the flow,

$$\partial c/\partial t + \boldsymbol{u}\cdot\nabla c = 0. \tag{1}$$

Thus the amount of contaminant contained in a lagrangian fluid element remains constant as the element moves through the flow. The evaluation of the mean concentration $\bar{c}$, ensemble averaged over different realizations of the turbulent flow, becomes now a problem of determining the probability density function that the fluid element at position $\boldsymbol{x}$ at time t originated at the point $\boldsymbol{a}$ when the contaminant was introduced. In this way

$$\bar{c}(\boldsymbol{x}, t) = \int c(\boldsymbol{a}, 0)\, p(\boldsymbol{X}(0) = \boldsymbol{a} \,|\, \boldsymbol{X}(t) = \boldsymbol{x})\, \mathrm{d}^3\boldsymbol{a}, \tag{2}$$

expressed in terms of the backwards probability distribution (Corrsin 1952). This

Phil. Trans. R. Soc. Lond. A (1990) **333**, 289–307
Printed in Great Britain

relation has prompted much work in the analysis of the lagrangian statistics of turbulent flows, of which some recent work is discussed in the companion paper by S. B. Pope (this issue).

In recent years effective stirring by chaotic advection has been observed even for laminar flows, a phenomenon sometimes referred to as lagrangian turbulence. Notable contributions in this subject have been made by Aref (1984), Chaiken *et al.* (1986), Dombre *et al.* (1986) and Ottino (1989) to mention but a few. This observation has broadened the range of contexts in which random stirring is considered and led to the development of new ideas about mixing in general. The position $\boldsymbol{X}(t)$ of a lagrangian fluid element is determined by the condition that the element moves with the local fluid velocity

$$\mathrm{d}\boldsymbol{X}/\mathrm{d}t = \boldsymbol{u}(\boldsymbol{x} = \boldsymbol{X}(t), t). \tag{3}$$

The dependence of fluid velocity on position is often nonlinear and complex, despite the apparent simplicity of (3). Viewed as a dynamical system (3) represents a nonlinear third-order system, which if the flow is unsteady is also non-autonomous. Such a system is ripe for chaos (Guckenheimer & Holmes 1983; Lichtenberg & Lieberman 1983) as found by Aref (1984) for an unsteady, two dimensional flow and by Dombre *et al.* (1986) for the steady, three-dimensional *ABC* flow. Characteristics of the irregular chaotic motion are sensitivity to the initial position of the fluid element and the rapid rate at which neighbouring elements separate. Viewed in this light chaotic advection may turn out to be a common feature. Steady, two-dimensional flows give rise only to a second-order, autonomous system which has regular solutions. As noted by Aref (1984), in these flows the stream function plays the role of a hamiltonian and the system is integrable. A review of recent work on the chaotic advection of fluid elements by Aref is included in this issue.

Another important aspect of mixing is the transport of small discrete particles by a flow. These particles may be solid aerosol particles in air, water droplets in air, spray droplets in a gas flow, crystals in a liquid melt, or vapour bubbles in liquids for example. Unlike a scalar contaminant these particles are not subject to molecular diffusion, though they may be influenced by brownian motion for very small sizes. The questions that now arise are: What is the average number of particles found in some sample volume? or What is the probability distribution for the number of particles? At low number densities and mass-loading (the mass of particles compared to the mass of fluid in some reference volume) the particles will have no dynamical influence on the flow and respond passively to the surrounding flow conditions. At low number densities the interactions of particles, such as coagulation through particle collisions, may be neglected and the transport of each particle may be considered separately. Under these conditions each particle retains its own identity.

The motion of small discrete particles is determined by the resultant force of the fluid on the particle, the effect of gravitational settling if important, and inertia. The response of a particle to the surrounding flow is more involved than the simple response of a lagrangian fluid element (3). This added complexity introduces new and interesting phenomena for the motion of particles in both laminar and turbulent flows. The aim of this paper is to review some specific features of the motion of small particles that have been found to occur, contrasting these with the comparable behaviour of lagrangian fluid elements. The discussion will be limited to laminar flows in which chaotic motion may or may not occur. The results are also indicative of the characteristics of particle motion in turbulence, though a discussion of this will not be included here.

PHILOSOPHICAL TRANSACTIONS OF THE ROYAL SOCIETY A MATHEMATICAL, PHYSICAL & ENGINEERING SCIENCES

In the first part of this paper the motion of spherical particles is considered, including the influence of gravitational settling and inertia, either of the particle or of the surrounding fluid. In the second part aspects of the motion of non-spherical particles are discussed, specifically for spheroidally shaped particles subject to gravitational settling. In both cases attention will be restricted to particles smaller in size than the smallest length scale of variation in the flow and sufficiently small that the relative motion of the particle to the surrounding fluid satisfies the conditions for a local Stokes flow. On the other hand the particles will be considered to be sufficiently large that brownian motion is not a significant factor. This may appear to be a narrow range of particle sizes but for say water droplets in low speed air flows, as in the atmosphere, would include particle radii of 5–50 μm. An excellent survey of particle characteristics is given by Clift *et al.* (1978), and a comprehensive review for atmospheric conditions is given by Pruppacher & Klett (1978).

2. Motion of a spherical particle

The motion of a small rigid sphere of mass m_p and radius a is governed by the balance of forces of the fluid on the particle, of gravity and the inertial acceleration of the particle. An equation of motion derived under general conditions for a non-uniform or unsteady flow (Maxey & Riley 1983) is

$$m_p \frac{d\boldsymbol{V}}{dt} = (m_p - m_F)\boldsymbol{g} + m_F \frac{D\boldsymbol{u}}{Dt} - \tfrac{1}{2} m_F \frac{d}{dt}(\boldsymbol{V} - \boldsymbol{u}(\boldsymbol{X}(t), t) - \tfrac{1}{10} a^2 \nabla^2 \boldsymbol{u}) - 6\pi a \mu \boldsymbol{Q}(t) - 6\pi a^2 \mu \int_0^t d\tau \frac{dQ/d\tau}{(\pi\nu(t-\tau))^{\frac{1}{2}}}, \quad (4)$$

where $\boldsymbol{V}(t)$ is the particle velocity, $\boldsymbol{X}(t)$ the position of the particle's centre and

$$\boldsymbol{Q}(t) = \boldsymbol{V}(t) - \boldsymbol{u}(\boldsymbol{X}(t), t) - \tfrac{1}{6} a^2 \nabla^2 \boldsymbol{u}. \quad (5)$$

In this equation of motion (4) $\boldsymbol{g}$ is the acceleration due to gravity, m_F is the mass of displaced fluid, and μ and ν are respectively the dynamic and kinematic viscosities of the surrounding fluid. The derivative $D\boldsymbol{u}/Dt$ is evaluated at the current particle position $\boldsymbol{X}(t)$ and is the acceleration of a corresponding fluid element in the ambient flow at this point. This term represents the fluid force on the particle from the undisturbed ambient flow. The other terms in (4) besides the effect of gravity and buoyancy represent the added-mass contribution, the Stokes drag force and the Basset history term modified appropriately (5) by the Faxen corrections for a non-uniform flow. This equation is based on the premise that the particle is much smaller than the length scale L for variation of the flow, $a/L \ll 1$ and that if U_0 is a velocity scale for the flow and W_0 a velocity scale for the relative motion of the particle to the surrounding fluid, the corresponding Reynolds numbers are small,

$$aW_0/\nu \ll 1, \quad a^2 U_0/L\nu \ll 1. \quad (6)$$

Associated with the inclusion of the Basset history term in the form here is the initial condition for the particle velocity that $\boldsymbol{Q}(t = 0)$ vanishes.

The response of a spherical particle as given by (4) is more complex than the simple motion of a lagrangian fluid element (3), with a variety of additional physical effects

included. For various situations this response is simpler. The mass of an aerosol particle, such as a spherical water droplet in air, is generally much greater than that of the displaced fluid. Terms involving m_F may be neglected and it is common practice for small particles to neglect the Faxen correction and Basset history term, unless one is concerned with the very initial stage of particle motion (Clift *et al.* 1978). The motion of an aerosol particle is given by

$$m_p \, d\boldsymbol{V}/dt = 6\pi a\mu(\boldsymbol{u}(\boldsymbol{X}(t), t) - \boldsymbol{V}(t)) + m_p \boldsymbol{g}, \tag{7}$$

where the dominant balance is of particle inertia, fluid drag force and gravitational settling. Although not strictly consistent it is convenient in determining the response of a general spherical particle also to neglect the Faxen and Basset terms and work with the simplified equation of motion

$$(m_p + \tfrac{1}{2}m_F)\, d\boldsymbol{V}/dt = (m_p - m_F)\boldsymbol{g} + 6\pi a\mu(\boldsymbol{u}(\boldsymbol{X}(t), t) - \boldsymbol{V}(t)) + \tfrac{3}{2}m_F \, \partial u/\partial t + m_F(\boldsymbol{u} + \tfrac{1}{2}\boldsymbol{V}) \cdot \nabla \boldsymbol{u}. \tag{8}$$

The assumption of low Reynolds number (6) leads to some arbitrariness in how the added-mass term is represented in (8) and other authors have used different forms (Auton 1983).

The discussion of spherical particles will be based on the equations of motion (7), (8). In still fluid a particle will eventually move with the Stokes settling velocity $\boldsymbol{W}^{(s)}$ determined by the equilibrium balance of gravitational settling and fluid drag forces

$$\boldsymbol{W}^{(s)} = (m_p - m_F)\boldsymbol{g}/6\pi a\mu. \tag{9}$$

The timescale on which the particle responds to changes in the local flow is determined by the inertia and drag forces and is given by $1/\alpha$, where

$$\alpha = 6\pi a\mu/(m_p + \tfrac{1}{2}m_F). \tag{10}$$

In terms of α, $\boldsymbol{W}^{(s)}$ and the mass ratio parameter R,

$$R = m_F/(m_p + \tfrac{1}{2}m_F), \tag{11}$$

the equation of motion (8) becomes

$$d\boldsymbol{V}/dt = \alpha[\boldsymbol{u}(\boldsymbol{X}(t), t) - \boldsymbol{V}(t) + \boldsymbol{W}^{(s)}] + \tfrac{3}{2}R \, \partial \boldsymbol{u}/\partial t + R(\boldsymbol{u} + \tfrac{1}{2}\boldsymbol{V}) \cdot \nabla \boldsymbol{u}. \tag{12}$$

This will allow us to consider both aerosol particles, m_F and R are both zero, and spherical vapour bubbles in liquids, m_p is zero and $R = 2$. That the Stokes drag law for a rigid sphere may be applied to a small bubble may be surprising. But it is common experience in anything but the cleanest liquids that surfactants accumulate on the bubble surface leading to a bubble rise velocity more accurately given by (9) than the corresponding Hadamard–Rybczinski result. This is discussed by Levich (1962).

A number of observations may be made directly on the basis of (12). First, the ratio of the inertial response time $1/\alpha$ to the timescale on which the local flow $\boldsymbol{u}(\boldsymbol{X}(t), t)$ changes determines the extent to which the particle responds to these changes. The non-dimensional ratio $\mathscr{A} = \alpha L/U_0$, or inverse of the Stokes number, is a useful indicator of this. For very large values of $\mathscr{A}$ the particle response is rapid and at each instant there is a quasi-steady balance, which from (12) is

$$\boldsymbol{V}(t) = \boldsymbol{u}(\boldsymbol{X}(t), t) + \boldsymbol{W}^{(s)}. \tag{13}$$

At each instant the particle velocity is the sum of the local fluid velocity and the Stokes settling velocity, and is simply a function of the particle position. This type of response is very similar to that of a lagrangian fluid element (3), as will be seen later.

Secondly, the motion of a spherical particle generally requires both the current position $\boldsymbol{X}(t)$ and velocity $\boldsymbol{V}(t)$ to be specified to evaluate the particle acceleration (12). A complete analysis involves the motion in a six-dimensional phase space of points $(\boldsymbol{X}(t), \boldsymbol{V}(t))$. Within this phase space the divergence,

$$\partial \dot{V}_i/\partial V_i + \partial V_i/\partial X_i = -3\alpha$$

is strictly negative indicating that the motion will eventually be restricted to some stable attractor set within the phase space. Physically this is consistent with the observation that in still fluid a particle will eventually settle at the Stokes settling velocity $\boldsymbol{W}^{(\mathrm{s})}$, whatever the initial particle velocity, or in a more general context that the particle motion has a limited sensitivity to the initial velocity.

Between these two one often encounters flows where the inertia parameter $\mathscr{A}$ has moderate to large values, where it is of some significance but not of major importance. It is then very useful to simplify (12) to obtain the particle velocity $\boldsymbol{V}$ again as a function of particle position alone while retaining a correction for inertia. A first approximation is that the particle velocity is given by (13), which substituted back into (12) yields the corrected form

$$\boldsymbol{V}(t) = \boldsymbol{u}(\boldsymbol{X}(t), t) + \boldsymbol{W}^{(\mathrm{s})} - \alpha^{-1}(\partial \boldsymbol{u}/\partial t + (\boldsymbol{u} + \boldsymbol{W}) \cdot \nabla \boldsymbol{u}) + (3R/2\alpha)\, \mathrm{D}\boldsymbol{u}/\mathrm{D}t + (R/2\alpha)\, \boldsymbol{W} \cdot \nabla \boldsymbol{u}. \quad (14)$$

The interesting feature that results from this specification (14) is that the divergence of the particle velocity field is non-zero even if the surrounding flow $\boldsymbol{u}$ is incompressible. The divergence is (Maxey 1987*a*)

$$\nabla \cdot \boldsymbol{V} = \alpha^{-1}(\tfrac{3}{2}R - 1)\left(\frac{\partial u_i}{\partial x_j}\frac{\partial u_j}{\partial x_i}\right), \quad (15)$$

and

$$\frac{\partial u_i}{\partial x_j}\frac{\partial u_j}{\partial x_i} = \frac{1}{4}\left(\frac{\partial u_i}{\partial x_j} + \frac{\partial u_j}{\partial x_i}\right)^2 - \frac{1}{4}\left(\frac{\partial u_i}{\partial x_j} - \frac{\partial u_j}{\partial x_i}\right)^2. \quad (16)$$

This divergence may be positive or negative. For a particle denser than the surrounding fluid, $m_{\mathrm{p}} > m_{\mathrm{F}}$ or $R < \frac{2}{3}$, the divergence is positive in regions of the flow dominated by high vorticity and negative in regions dominated by high strain rate. There is then a bias mechanism and in any flow the particles will tend to accumulate in regions of high strain rate. Conversely, particles such as bubbles which are less dense than the surrounding fluid, $m_{\mathrm{p}} < m_{\mathrm{F}}$, will have a divergence of the opposite sign and show a tendency to accumulate in regions of high vorticity. This bias mechanism has been noted for aerosol particles by Maxey (1987*b*) and by McLaughlin (1988), Fernández de La Mora & Riesco-Chueca (1988), among others. It is linked to how quickly a particle with inertia may turn in following a curved path in the flow. It is easily illustrated by considering how a particle would move close to an isolated vortex core or in a region of pure straining flow. This behaviour is in contrast to the motion of lagrangian fluid elements which show no such bias in an incompressible flow, or of those particles with negligible inertial effects (13).

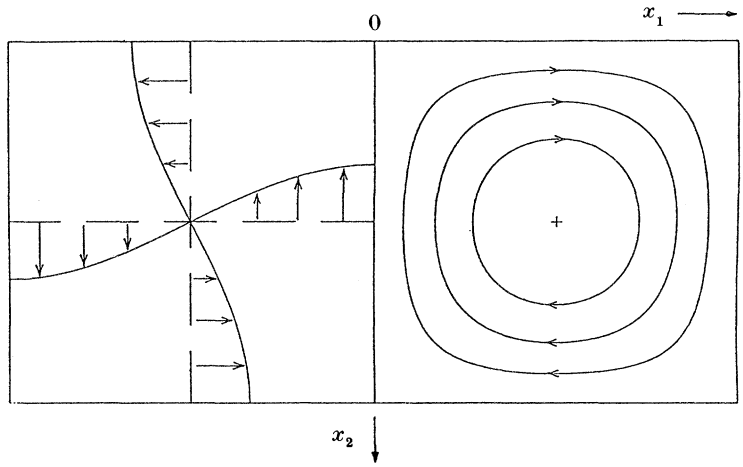

Figure 1. Sketch of the velocity profiles for the left-hand cell, and streamlines for the right-hand cell, of the periodic cellular flow field. Arrows show the direction of flow.

3. Spherical particles in a cellular flow

The significance of these mechanisms on the motion of spherical particles is best understood by considering the motion in some specific flows. In this paper the steady two-dimensional flow specified by the stream function $\psi(x_1, x_2)$ for a cellular flow,

$$\psi(x_1, x_2) = U_0 L \sin(x_1/L) \sin(x_2/L) \tag{17}$$

is used as a standard example. The streamlines and an outline of the velocity profile are shown in figure 1. The flow extends periodically in both x_1 and x_2 directions, and satisfies the inviscid Euler equations for steady flow. The flow (7) is also found in thermal convection with free-slip boundaries. A lagrangian fluid element (3) introduced into this flow will follow a simple, closed path corresponding to some streamline of the steady flow and the value of ψ will be a constant of the motion.

Stommel (1949) gave results for the motion of spherical particles, with negligible inertia yet subject to gravitational settling. The motion of these particles is governed by (13) and is regular like that of the fluid elements. The main observation Stommel made was that for cells aligned vertically, so that $\boldsymbol{g}$ is parallel to the x_2-axis and $\boldsymbol{W}^{(s)}$ is $(0, W^{(s)})$, some particles may be held indefinitely in suspension by the flow provided the maximum upflow, U_0 exceeds the terminal fall speed $W^{(s)}$ as given in (9). Some particle paths are shown in figure 2. The particles retained in the flow follow closed paths, being swept up by the flow near the cell boundary at $X_1 = 0$. There are static equilibrium points along $X_1 = 0$ at points where $X_2 = L \arcsin(W^{(s)}/U_0)$, of which there are two in the cell shown. There is a bounding path emanating from the equilibrium points separating the flow into two regions, one where particles are suspended and the other where particles settle out along open paths. The extent of the suspension region decreases as $W^{(s)}/U_0$ approaches unity.

The motion of aerosol particles (7) in the cellular flow (17) has been studied by Maxey & Corrsin (1986) and for more general spherical particles (12) by Maxey (1987*a*). Some of the main results are included here, and these references may be consulted for further details. The first observation is that aerosol particles are no longer suspended by the flow, rather particles spiral out of the upflow regions and all eventually settle through the downflow regions of successive cells. Sample particle

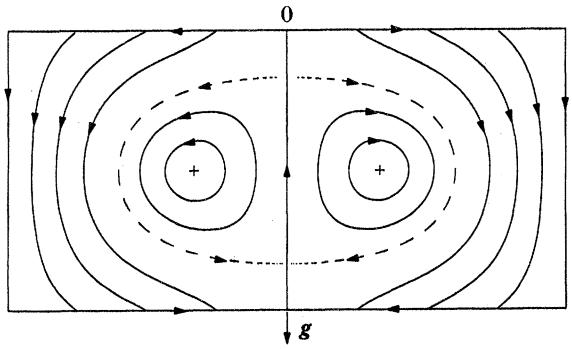

Figure 2. Trajectories of spherical particles settling under gravity in the cellular flow field according to (13), without inertial effects. $W^{(s)}/U_0 = 0.5$; broken line shows bounding trajectory for the trapping region. Arrows on the cell boundaries indicate the circulation in each cell.

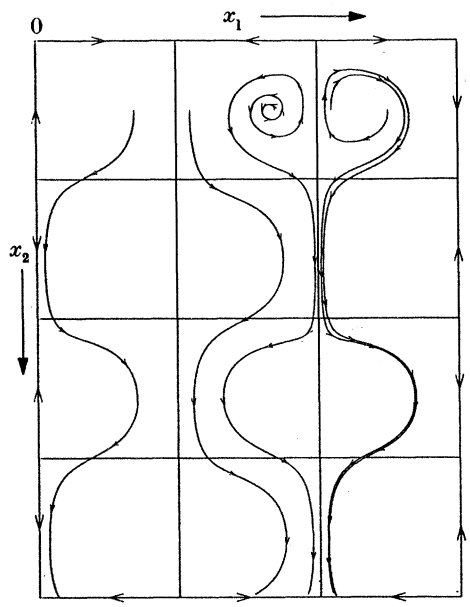

Figure 3. Sample trajectories for aerosol particles ($R = 0$) settling under gravity in a cellular flow. Stokes settling velocity $W^{(s)} = 0.5U_0$, inertia parameter $A = 5$. The arrows on the trajectories are drawn at intervals of $2L/U_0$; the arrows on the cell boundaries indicate the circulation in each cell.

trajectories are shown in figure 3. The second observation is that eventually all the particle trajectories merge into isolated paths which settle through the cells. This feature is illustrated by the particle position plot shown in figure 4. To obtain this plot particles were introduced into the flow on a regular 10×10 grid of equally spaced mesh points within each cell and their motion followed. This position of each particle was plotted at $t = 80L/U_0$, and use was made of the periodic nature of the flow to reduce the position coordinates to lie in the range $0 \leqslant x_1, x_2 \leqslant 2\pi L$. The plot shows how the particles have accumulated along narrowly defined curves. At later times the position plots have the same character and are more sharply defined. This indicates an asymptotic convergence, and since the particles remain on these curves subsequently the curves correspond to segments of an asymptotic particle trajectory.

PHILOSOPHICAL TRANSACTIONS OF THE ROYAL SOCIETY A MATHEMATICAL, PHYSICAL & ENGINEERING SCIENCES

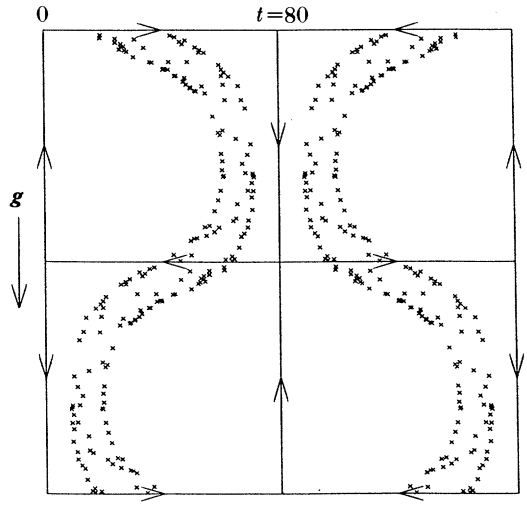

Figure 4. Particle position plots at $t = 80L/U_0$ for an initially uniform array of particles settling under gravity; $W^{(s)} = 0.5U_0$, $\mathscr{A} = 5$, $R = 0$.

The tendency for aerosol particles to accumulate along selected paths was found to be a general feature for a wide range of parameters. Particles, whose Stokes settling velocity $W^{(s)}$ exceeded U_0 tended to collect along the vertical cell boundaries and settle out along these. Even as particle inertia was reduced, increasing the value of $\mathscr{A}$, the same tendency developed only taking longer to become established. The same features were obtained using either the full equation (7) or the corresponding approximate form (14) with $R = 0$. The same general behaviour was further observed for general spherical particles (12) which were more dense than the surrounding fluid, $m_p > m_F$.

The bubble particles, $m_p = 0$, or $R = 2$, had a somewhat different response to the cellular flow. Unlike aerosol particles, bubble particles tend to rise through a fluid. After taking account of this change in the Stokes velocity (9), one finds as before that if the flow speed U_0 exceeds $|\boldsymbol{W}^{(s)}|$ there are static equilibrium points for the bubbles, this time in the downflow regions of the cells. Along $X_1 = 0$, equilibrium points exist at values of x_2 where

$$|\boldsymbol{W}^{(s)}|/U_0 = -\sin(X_2/L) + R/\mathscr{A}\sin(X_2/L)\cos(X_2/L).$$

These points are unstable for all values of R. Within each cell there is an interior equilibrium point, which is marked in figure 2 for the particle without inertia. This equilibrium point is linearly stable for a bubble particle but unstable for an aerosol particle. The stability of these interior points is illustrated by the sample particle trajectories of figure 5, where it is evident that particles are moving closer to these points and being permanently trapped. Also shown are bubbles rising continuously through the cellular flow.

A particle position plot corresponding to figure 4, but for bubble particles is shown in figure 6. Here the flow speed exceeds the bubble rise velocity and four interior equilibrium points are evident in the diagram. A substantial number of particles have been trapped at these equilibrium points, while the others continue to rise and accumulate along isolated curves rising through the cell. For more rapidly rising

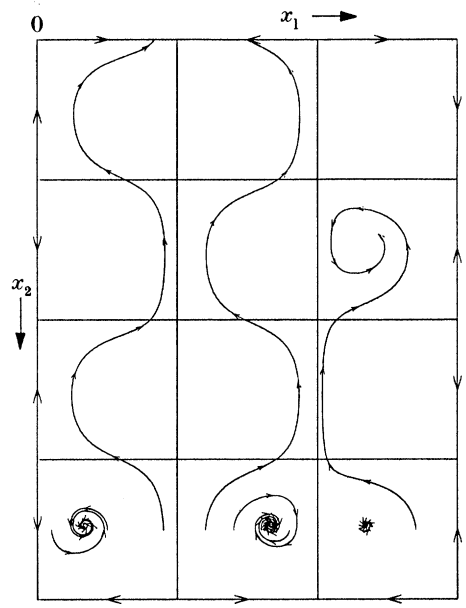

Figure 5. Sample trajectories for bubble particles ($R = 2$) rising through the cellular flow field due to buoyancy. Stokes terminal speed $|\boldsymbol{W}^{(s)}| = 0.5U_0$ for bubble rise, inertia parameter $\mathscr{A} = 10$. Arrows on the trajectories are drawn at intervals of $2L/U_0$.

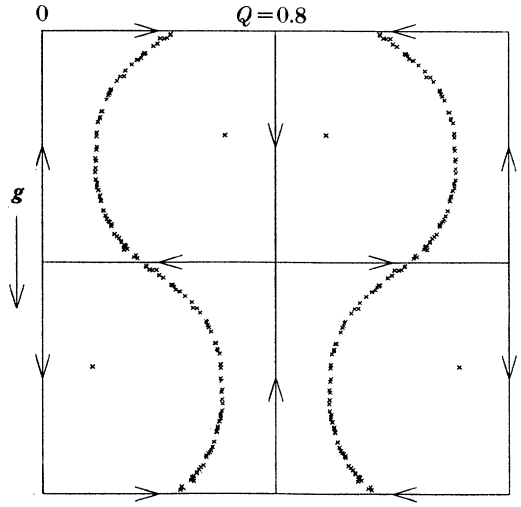

Figure 6. Particle position plots at $t = 100L/U_0$ for an initially uniform array of bubble particles ($R = 2$). Stokes terminal rise speed $|\boldsymbol{W}^{(s)}| = 0.8U_0$, inertia parameter $\mathscr{A} = 10$.

bubbles, no equilibrium points are possible and all the particles collect along such isolated curves, rising through the cell.

In summary, at this point, it is apparent that the inertia associated with the particle motion leads to the tendency for the individual trajectories of spherical particles to merge into isolated paths. There is organization of the motion through the bias mechanisms noted in (15) and (16), which goes beyond what may otherwise be expected to occur simply due to inertia.

It may be noted that the vorticity of the cellular flow is strongest towards the centre of each cell, while the rate of strain dominates on the cell boundaries. The stability of the interior equilibrium points for a bubble is consistent with the bias mechanism and the effect of vorticity. The vortex trapping of bubbles through the influence of added-mass effects has been reported by Auton (1983) and Thomas *et al.* (1983, 1984).

4. Spherical particles and lagrangian turbulence

The cellular flow field just considered was a steady, two-dimensional flow with regular motion of the lagrangian fluid elements. The response of the spherical particles was similarly regular with a further high degree of organization to the particle trajectories. As it has been observed that several unsteady or three-dimensional laminar flows have been found to produce chaotic motion of the lagrangian fluid elements, an interesting question is whether spherical particles would be similarly affected by such a flow.

One study by Smith & Spiegel (1985) considered the motion of sedimenting particles for which inertial effects were negligible. They examined the motion of spherical particles given by (13) in an unsteady cellular flow field specified by the stream function

$$\psi(x_1, x_2, t) = (1/\pi)\,[1+\epsilon\cos(\sigma t)]\sin(\pi x_1)\sin(\pi x_2), \tag{19}$$

as opposed to the steady flow (17). This system is hamiltonian, with one degree of freedom and the particle stream function ϕ, defined by

$$\phi = \psi - W^{(s)}\,x_1, \tag{20}$$

and where

$$\mathrm{d}X_1/\mathrm{d}t = \partial\phi/\partial x_2, \quad \mathrm{d}X_2/\mathrm{d}t = -\partial\phi/\partial x_1 \tag{21}$$

plays the role of a hamiltonian (Aref 1984). For non-zero values of ϵ and σ the flow is unsteady and the hamiltonian time-dependent, which introduces then the possibility of chaotic motion. This was indeed observed and the flow was found to contain islands of regular motion where particles were permanently retained, outside of which the particles settled in a chaotic manner. The authors found similar behaviour for a range of values of ϵ and σ, and further analysed the fractal nature of initial clusters of particles as they are advected by the flow. Unsteady flows similar to (19) have been observed by Solomon & Gollub (1988) for unsteady rolls in experiments on thermal convection between horizontal plane boundaries. They have also reported on the chaotic advection of fluid elements in such flows.

The inclusion of gravitational settling alone, as in (13), produces particle motion very similar to that of lagrangian fluid elements except that the flow is changed by the addition of a uniform, constant velocity $\boldsymbol{W}^{(s)}$. The methods of analysis and the sources of chaotic motion are essentially equivalent.

More recently McLaughlin (1988) has examined the motion of spherical particles in the three-dimensional *ABC* flow of Arnold (1965), including both gravitational settling and inertial effects. The *ABC* flows are steady, incompressible solutions of the Euler equations and are examples of Beltrami flow for which the vorticity and velocity vectors are parallel to each other. The flow is

$$u_1 = A\sin(2\pi x_3) + C\cos(2\pi x_2), \tag{22a}$$

$$u_2 = B\sin(2\pi x_1) + A\cos(2\pi x_3), \tag{22b}$$

$$u_3 = C\sin(2\pi x_2) + B\cos(2\pi x_1). \tag{22c}$$

The standard condition $1 = A \geqslant B \geqslant C \geqslant 0$ is usually applied. Dombre *et al.* (1986) have found for a range of parameter values of B, C that this flow leads to the chaotic advection of fluid elements. For the specific value of $C = 0$ the system is integrable and there is no chaotic advection. The flow consists of six principal vortices, two of which are aligned in each of the three directions. As C is increased regions of chaotic advection are observed in the flow.

In this study McLaughlin (1988) considered particles subject only to weak inertial effects such that the departures in the particle velocity from the local fluid velocity could be represented by an equation similar to (14). This approximate representation was derived from (12) with the additional approximation that $\mathrm{D}\boldsymbol{u}/\mathrm{D}t$ was equal to $\mathrm{d}\boldsymbol{u}/\mathrm{d}t$ to the degree of accuracy of the Stokes flow assumption (6). This leads to the modified form of (12)

$$\mathrm{d}\boldsymbol{V}/\mathrm{d}t = \alpha[\boldsymbol{u}(\boldsymbol{X}(t), t) - \boldsymbol{V} + \boldsymbol{W}^{(\mathrm{s})}] + \tfrac{3}{2}R\,\mathrm{d}\boldsymbol{u}/\mathrm{d}t,$$

which in turn leads to the modified approximate form for weak inertial effects

$$\boldsymbol{V} = \boldsymbol{u}(\boldsymbol{X}(t), t) + \boldsymbol{W}^{(\mathrm{s})} + \alpha^{-1}(\tfrac{3}{2}R - 1)\,\mathrm{d}\boldsymbol{u}/\mathrm{d}t, \tag{23}$$

in the present notation. With length and velocity scales implied by (22) and the condition $A = 1$, the group $\alpha^{-1}(\frac{3}{2}R - 1)$ corresponds to the parameter $\gamma/2\pi$ used by McLaughlin.

Without gravitational settling a flow exhibiting lagrangian turbulence, $B^2 = 0.5001$ and $C^2 = 0.0002$, led to the eventual capture of bubble-like particles by one of the principal vortices. The value of γ was 0.0628. This is similar to the vortex capture of bubbles discussed at the end of the last section and noted by Thomas *et al.* (1983, 1984). No persistent chaotic motion was observed. For aerosol particles or particles more dense than the fluid, $\gamma = -0.0628$, chaotic motion was only observed for very limited ranges of values of B and C. Generally chaotic motion was transient and the particles were captured by periodic or quasiperiodic trajectories. No chaotic attractors were found for $(B^2 + C^2) < 1$.

With the introduction of gravitational settling, but no inertia ($\gamma = 0$), limited regions of permanent particle suspension were possible, surrounding by larger regions where particles settled out in a chaotic motion. With the inclusion of inertia ($\gamma = -0.0628$) these regions of permanent suspension disappeared, as was found for the steady cellular flow. Similarly the chaotic sedimentation was eliminated for most values of B, C and the particle trajectories converged to asymptotic periodic or quasiperiodic paths. Interestingly some of these asymptotic paths may hold a particle in permanent suspension within the flow.

The results of this study indicate that inertial effects of the particle eliminate, or severely reduce, the chaotic advection of fluid elements at least in the limit of weak particle inertia. This is supported by some results of Wang *et al.* (1990) also for the *ABC* flow system. This may well be true of other flows exhibiting lagrangian turbulence, yet this remains to be established.

5. Motion of non-spherical particles

Departures from a spherical shape introduce new features to the motion of a particle. One must find not only the velocity of the particle but also the angular velocity $\boldsymbol{\Omega}(t)$ to determine the motion. Further the particle orientation is coupled to

PHILOSOPHICAL TRANSACTIONS OF THE ROYAL SOCIETY A MATHEMATICAL, PHYSICAL & ENGINEERING SCIENCES

the particle velocity through changes in the gravitational settling velocity. The simplest non-spherical shape to consider is that of an orthotropic, axisymmetric particle of which the spheroid or ellipsoid of revolution is an example. The motion of a small neutrally buoyant ellipsoid in a steady uniform shear flow was studied by Jeffery (1922), who developed the equations governing the particle rotation in a flow with uniform velocity gradients. Extension to these results are given by Bretherton (1962) and Happel & Brenner (1965) for particles within the Stokes régime.

When a small, isolated rigid particle is introduced into a flow field $\boldsymbol{u}(\boldsymbol{x},t)$, it produces a local disturbance flow $\boldsymbol{v}(\boldsymbol{x},t)$ such that the sum of the two forms the resultant flow. Away from the particle $\boldsymbol{v}$ becomes negligible while on the particle surface $(\boldsymbol{v}+\boldsymbol{u})$ must satisfy no-slip boundary conditions. For sufficiently small particles the variations in $\boldsymbol{u}$ over the particle surface are well represented by the local value of $\nabla\boldsymbol{u}$, or equivalently the local fluid vorticity $\boldsymbol{\omega}$ and rate of strain tensor $\boldsymbol{E}$. Under conditions similar to (6) the disturbance flow $\boldsymbol{v}$ is a Stokes flow and the resultant fluid force $\boldsymbol{F}$ on the particle is linearly related to the relative velocity of the particle to the surrounding fluid, $(\boldsymbol{V}-\boldsymbol{u}(\boldsymbol{X}(t),t))$ and to $\boldsymbol{\omega}(\boldsymbol{X}(t),t)$ and $\boldsymbol{E}(\boldsymbol{X}(t),t)$. The resultant fluid torque $\boldsymbol{G}$ on the particle is similarly related. The reflexional symmetry of orthotropic particles leads to

$$F_i = \mu K_{ij}(u_j(\boldsymbol{X}(t),t) - V_j(t)), \tag{24}$$

$$G_i = \mu R_{ij}(\tfrac{1}{2}\omega_j - \Omega_j) + \mu D_{ijk} E_{jk}, \tag{25}$$

where $\boldsymbol{R}$ and $\boldsymbol{K}$ are symmetric and $\boldsymbol{D}$ is a pseudo-tensor symmetric in j, k (Happel & Brenner 1965). For particles of uniform composition the principal axes of $\boldsymbol{R}$ and $\boldsymbol{K}$ coincide with the symmetry axes of the particle, which for an axisymmetric particle consist of the unit vector $\boldsymbol{m}$ parallel to the axis of symmetry and two orthogonal unit vectors normal to $\boldsymbol{m}$.

Consistent with the assumption of quasi-steady Stokes flow for $\boldsymbol{v}$ no account will be made here of the effects of particle or fluid inertia. The particle response to changes in the local flow conditions is assumed to be rapid, equivalent to that leading to (13), and the motion is determined by the conditions that at each instant the net force $\boldsymbol{F}+m\boldsymbol{g}$ on the particle, and the net torque $\boldsymbol{G}$ vanish. The former leads to the specification of the particle velocity as

$$\boldsymbol{V}(t) = \boldsymbol{u}(\boldsymbol{X}(t),t) + W_1(\hat{\boldsymbol{g}}\cdot\boldsymbol{m})\,\boldsymbol{m} + W_2(\hat{\boldsymbol{g}} - \hat{\boldsymbol{g}}\cdot\boldsymbol{m}\boldsymbol{m}), \tag{26}$$

where $\hat{\boldsymbol{g}}$ is the unit vector $\boldsymbol{g}/|\boldsymbol{g}|$. In still fluid the particle has two principal fall speeds, W_1 for settling parallel to the axis of symmetry and W_2 for settling transverse to the symmetry axis. In general W_1 and W_2 differ from each other, and the particle velocity $\boldsymbol{V}$ (26) is coupled to the orientation $\boldsymbol{m}$ through this difference. In the absence of gravitational settling the particle moves with the local fluid velocity.

The rotation of the particle is specified by the condition of no net torque

$$\mathrm{d}\boldsymbol{m}/\mathrm{d}t = \boldsymbol{\Omega}\times\boldsymbol{m}, \tag{27}$$

$$\boldsymbol{\Omega}(t) = \tfrac{1}{2}\boldsymbol{\omega}(\boldsymbol{X}(t),(t) + D\boldsymbol{m}\times(\boldsymbol{E}\cdot\boldsymbol{m}). \tag{28}$$

The particle turns in response to both the local vorticity and the local rate of strain. In a flow that is purely rotational, $\boldsymbol{E}=0$, the particle will rotate indefinitely; but in an irrotational straining flow will rotate only until the symmetry axis is aligned with one of the principal axes of strain-rate.

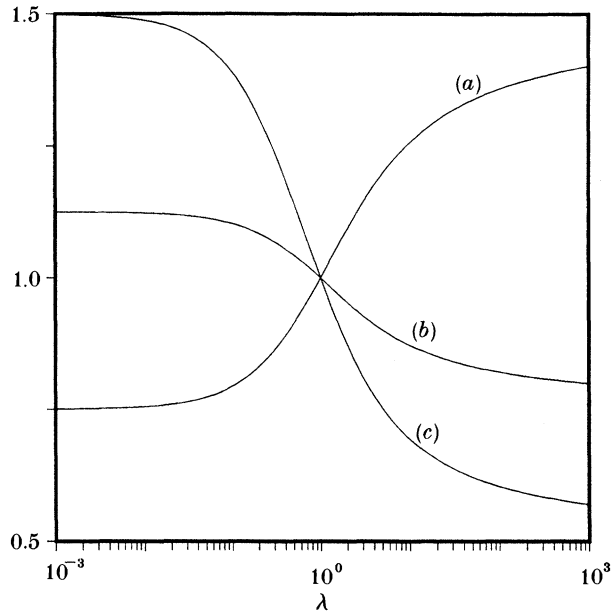

Figure 7. The ratio of the terminal fall speeds $\Lambda = W_2/W_1$ for a spheroidal particle with aspect ratio λ. The ratio $\lambda = 1$ for a sphere, $\lambda < 1$ for an oblate spheroid and $\lambda > 1$ for a prolate spheroid. Results based on Stokes flow solutions. (*a*) W_1/W_2; (*b*) W_2/V_∞; (*c*) Λ.

Values for the parameters W_1, W_2 and D may be assigned for spheroidal particles in terms of the aspect ratio λ using standard relations (Bretherton, 1962). These are shown in figure 7 for both prolate ($\lambda > 1$) and oblate ($\lambda < 1$) shapes. The spherically averaged fall speed V_∞, for a particle of random orientation is introduced

$$V_\infty = \tfrac{1}{3}(W_1 + 2W_2). \tag{29}$$

The value of D is

$$D = (\lambda^2 - 1)/(\lambda^2 + 1). \tag{30}$$

This is positive for a prolate shape indicating that the spheroid will turn in an irrotational flow till the axis $\boldsymbol{m}$ is aligned with the direction of greatest positive strain-rate. The divergence of the velocity in the phase $(\boldsymbol{X}(t), \boldsymbol{m}(t))$ reflects this preferred alignment and is equal to $(-5D\boldsymbol{m}\cdot\boldsymbol{E}\cdot\boldsymbol{m})$.

In a steady, uniform shear flow, without gravitational settling, Jeffery (1922) showed that the particles rotate in a regular periodic manner. The equations (27), (28) for particle rotation are formally third order, but the constraint that $\boldsymbol{m}$ is a unit vector means that there are only two independent equations. Under steady uniform conditions, where $\boldsymbol{\omega}$ and $\boldsymbol{E}$ are constants, the possibility of chaotic orientations is thus precluded.

6. Non-spherical particles in a cellular flow

In this section we now consider the motion of sedimenting nonspherical particles in the cellular flow (17) discussed previously. Here I draw on the preliminary results reported by Mallier & Maxey (1990) and the more recent work by Shin (1990). The particle motion is specified by the equations (26)–(28) for $\boldsymbol{V}(t)$ and the orientation

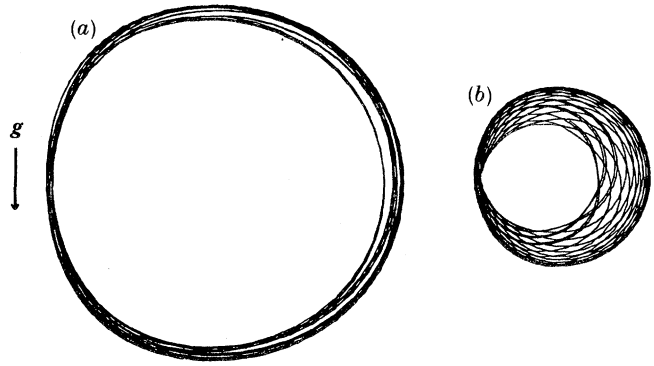

Figure 8. The trajectory of a spheroidal particle suspended by the cellular flow within the region $0 \leqslant x_1, x_2 \leqslant 1$: (*a*) aspect ratio $\lambda = 2$, spherically averaged fall speed $V_\infty = 0.25$, particle introduced at $(X_1, X_2) = (0.6875, 0.4375)$; (*b*) $\lambda = 10$, $V_\infty = 0.25$, particle initial position (0.5625, 0.4375).

$\boldsymbol{m}(t)$ with the fluid velocity, vorticity and rate of strain corresponding to (17). The direction of $\hat{\boldsymbol{g}}$ is taken to be in the positive x_2-direction, as before, for vertically aligned cells. The scales L, U_0 in (17) are chosen to be $1/\pi$, 1 respectively. The full system is quite complex and contains many new features. To obtain a better physical understanding of the processes a restricted problem is considered where $\boldsymbol{m}$ is constrained to lie in the x_1, x_2-plane with $m_3 = 0$. Mallier & Maxey (1990) have noted that if m_3 is zero initially then the axis will remain in the plane thereafter, and further that V_3 is zero. Preliminary computations, supported by the later work of Shin (1990), showed that the results of the restricted planar motion were similar in character to that of the full system.

The particle orientation $\boldsymbol{m}$ may be characterized by the angle θ that the particle axis make with the x_1-axis in this restricted system. The components of $\boldsymbol{m}$ are $(\cos\theta, \sin\theta, 0)$ and the equations governing the motion are

$$V_1 = \sin \pi X_1 \cos \pi X_2 + (W_1 - W_2) \sin\theta \cos\theta, \tag{31}$$

$$V_2 = -\cos \pi X_1 \sin \pi X_2 + W_2 + (W_1 - W_2) \sin^2\theta, \tag{32}$$

$$\mathrm{d}\theta/\mathrm{d}t = \pi \sin \pi X_1 \sin \pi X_2 - 2D\pi \cos \pi X_1 \cos \pi X_2 \sin\theta \cos\theta. \tag{33}$$

The first difference from the motion of spherical particles, discussed in §3, is that now at an equilibrium point the particle may not turn. This eliminates the equilibrium points in the interior of the cells, and along the $X_1 = 0$ cell boundary equilibrium points exist at points where $\sin \pi X_2 = W_2$ for $\theta = 0$, or at $\sin \pi X_2 = W_1$ for $\theta = \frac{1}{2}\pi$. Previously the particle orientation was of no significance. For a sphere W_1, W_2 are the same. The permanent suspension of spheroidal particles by the flow, similar to that shown in figure 2, is still possible. This is illustrated by the regular paths in the x_1, x_2-plane shown by figure 8. The paths are no longer simple closed curves, but show the effects of the particle turning in response to the local vorticity and rate of strain, and the influence of this back on the particle velocity. The region of the flow supporting particle suspension is significantly reduced.

Outside of the suspension regions particles generally exhibit a chaotic tumbling motion. The paths in the x_1, x_2-plane and the corresponding particle orientations of typical particles settling through the flow are shown in figure 9. For a spherical particle settling through the flow the path is periodic in the x_2-direction, but the orientation is quasi-periodic due to the variations in vorticity and rate of strain in

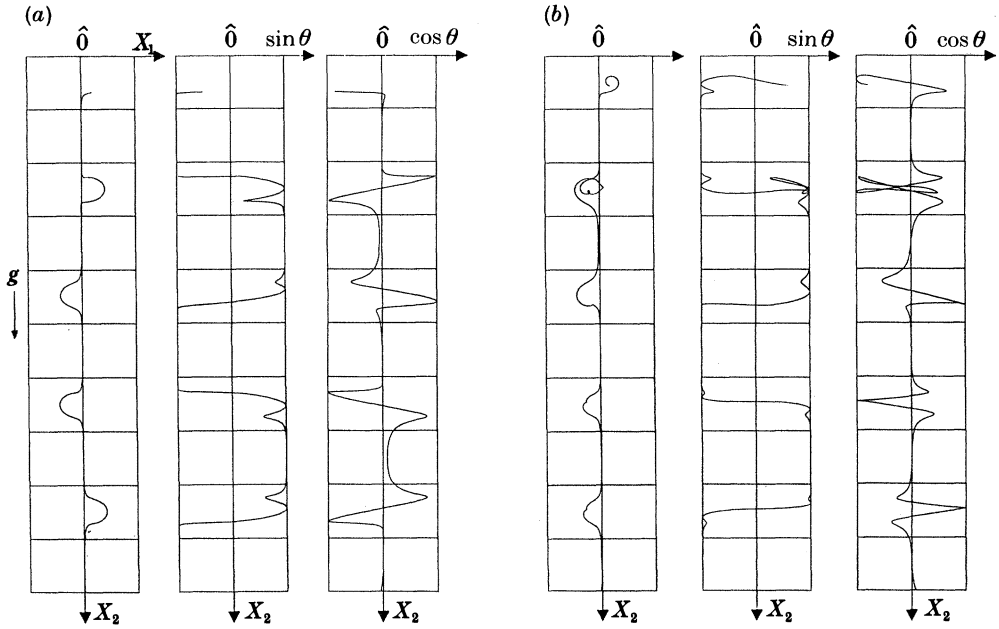

Figure 9. The trajectory of a spheroidal particle settling through the cellular flow showing the path (X_1, X_2) and particle orientation $\boldsymbol{m} = (\cos\theta, \sin\theta)$: (*a*) aspect ratio $\lambda = 2$, $V_\infty = 0.75$; (*b*) $\lambda = 10$, $V_\infty = 0.75$. Boxes drawn to mark unit cells.

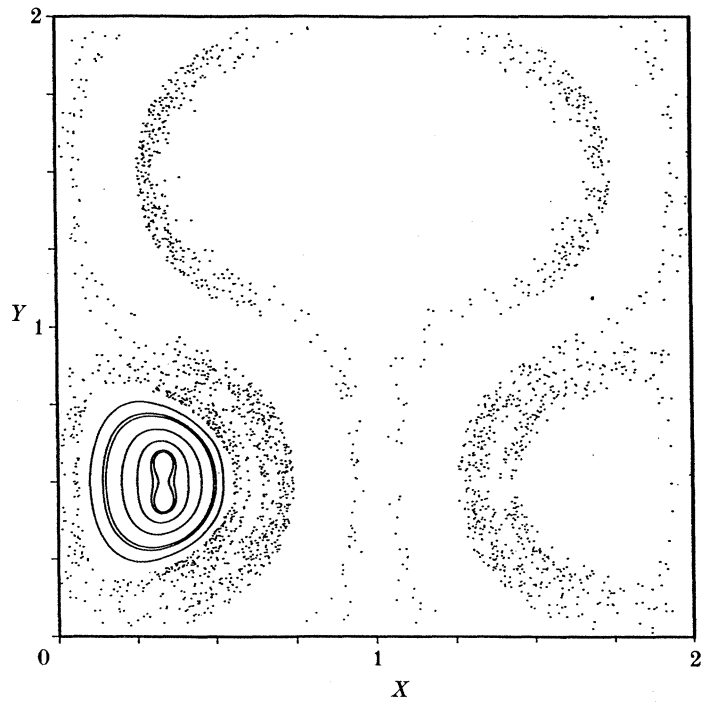

Figure 10. Poincaré sections for non-spherical particles subject to gravitational settling with principal fall speeds $W_1 = 0.5$ and $W_2 = 0.4$. No coupling with the rate of strain, $D = 0$. Sections based on intersections with $\theta = 0$. Note that the X_2-axis is now drawn up the page.

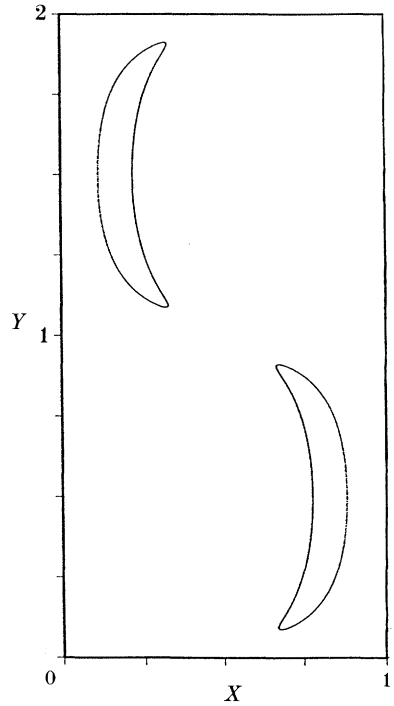

Figure 11. Poincaré section for the same conditions as figure 10 showing intersection points for a particle in the regular settling region.

(33). For a spheroidal particle the coupling of orientation and velocity leads to a chaotic behaviour in this region of the flow. This is confirmed by the broad spectrum of the time series for $m_1(t)$.

Shin (1990) has found that chaotic tumbling is still a feature of the particle motion even if D is zero and the particle turns only in response to the local vorticity. The character of the motion appears to be much the same. The system of equations (31)–(33) are however now volume preserving in phase space. The Poincaré section for such a system based on the intersections with $\theta = 0$ (figure 10) shows quite well the region of the flow where particles are suspended and have regular motion. Outside this region the chaos is clearly evident. The intersection points in this latter part of the flow were generated by a single particle trajectory with explicit use being made of the periodicity of the flow. Of interest is that the particle trajectories passing close to the $x_1 = 0$ cell boundary are chaotic. In figure 10 there are clear bands where no intersection point was found. A separate Poincaré section for this region (figure 11) shows that there is regular motion here and the particles settle without chaotic tumbling. Within the region of regular motion noted here the Lyapunov exponents were found to be indeed zero asymptotically, while in the region of chaotic tumbling positive exponent values were obtained.

The assertion that the general character of the motion is similar whether D is zero or not may be viewed by a comparison of the Poincaré sections of figure 12. These were obtained for identical conditions except that in the first $D = 0$ while in the second $D = 0.5$. Evident are the regions of chaotic settling, regular particle suspension and regular particle settling.

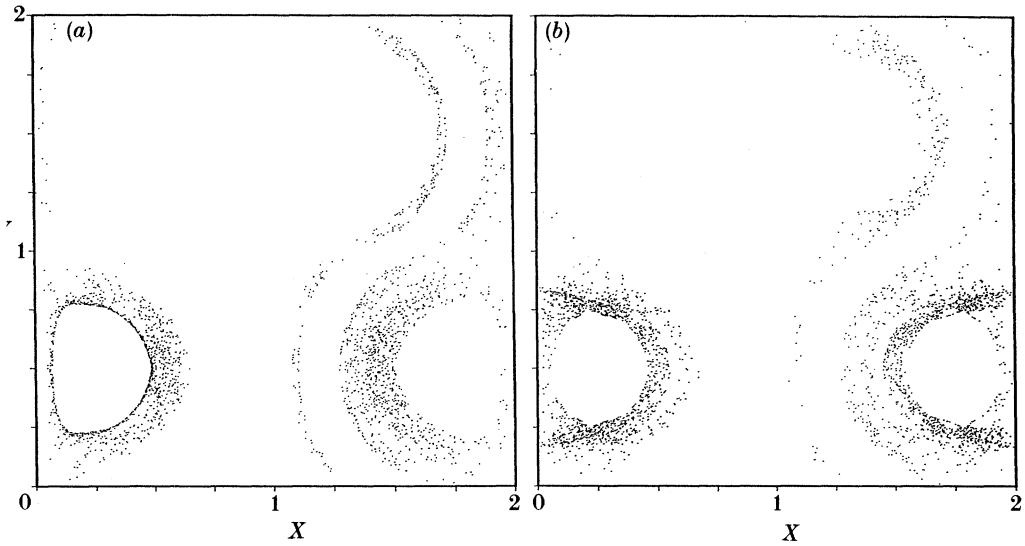

Figure 12. Poincaré sections for non-spherical particles intersecting at $\theta = 0$, showing the influence of strain-rate coupling. Principal fall speeds $W_1 = 0.6$, $W_2 = 0.5$. Initial points at $X_1 = 0.05$, $X_2 = 0.5$, $\theta = 0$: (*a*) $D = 0$, (*b*) $D = 0.5$.

The results summarized here suggest that for the cellular flow field chaotic settling will be a feature of all non-spherical motion, with regions of regular motion for particle suspension and regions associated with regular settling motion. The extent of each of these will depend on the aspect ratio of the particle and the departure from a spherical shape. The motion of a sphere is of course completely regular. Further work will be required to substantiate this picture.

7. Conclusion

Several features of the motion of discrete spherical and non-spherical particles have been discussed here and how these compare with the motion of lagrangian fluid elements. In the cellular flows the motion of both lagrangian fluid elements and spherical particles was regular, with the influence of inertial effects leading to an organized structure of preferred particle trajectories. The motion of non-spherical particles, subject to gravitational settling but not to inertial effects, by contrast could be chaotic. In the *ABC* flows inertial effects on the motion of spherical particles produced regular particle trajectories eventually, even if the motion of lagrangian fluid elements was chaotic. The general features that seem to be emerging are that inertial effects, when they are weak or moderate, inhibit chaotic mixing while tumbling due to a non-spherical shape promotes chaotic mixing. Some evidence, however, was found in the results of Maxey & Corrsin (1986) that very strong particle inertia may also promote disorganized particle motion. In any given flow system it would appear that a range of behaviour is possible depending on the response of the particle to the surrounding flow conditions.

Beyond their immediate contexts, the results given here indicate features of particle motion that may be expected to occur in other more complex flow systems, such as turbulent flows.

PHILOSOPHICAL TRANSACTIONS OF THE ROYAL SOCIETY A MATHEMATICAL, PHYSICAL & ENGINEERING SCIENCES

I express my gratitude to Roland Mallier and Hyundoo Shin for their substantial contributions to the work on non-spherical particle motion, and for their collaboration. The support from the DARPA-URI Program under contract number ONR-N00014-86-K0754 is gratefully acknowledged.

References

Aref, H. 1984 Stirring by chaotic advection. *J. Fluid Mech.* **143**, 1–21.

Arnold, V. I. 1965 Sur la topologie des écoulements stationnaires des fluids parfaits. *C.r. hebd. Seanc. Acad. Sci., Paris* **261**, 17–20.

Auton, T. R. 1983 The dynamics of bubbles, drops and particles in motion in liquids. Ph.D. dissertation, University of Cambridge, U.K.

Batchelor, G. K. 1949 Diffusion in a field of homogeneous turbulence. I, Eulerian analysis. *Aust. J. Sci. Res.* **2**, 437–450.

Batchelor, G. K. & Townsend, A. A. 1956 Turbulent diffusion. In *Surveys in mechanics* (ed. G. K. Batchelor & R. M. Davies), pp. 352–399. Cambridge University Press.

Bretherton, F. P. 1962 The motion of rigid particles in a shear flow at low Reynolds number. *J. Fluid Mech.* **14**, 284–304.

Chaiken, J., Chevray, R., Tabor, M. & Tan, Q. M. 1986 Experimental study of Lagrangian turbulence in a Stokes flow. *Proc. R. Soc. Lond.* A **408**, 165–174.

Clift, R., Grace, J. R. & Weber, M. E. 1978 *Bubbles, drops and particles.* New York: Academic.

Corrsin, S. 1952 Heat transfer in isotropic turbulence. *J. appl. Phys.* **23**, 113.

Dombre, T., Frisch, U., Greene, J. M., Henon, M., Mehr, A. & Soward, A. M. 1986 Chaotic streamlines in the ABC flows. *J. Fluid Mech.* **167**, 353–391.

Fernández de la Mora, J. & Riesco-Chueca, P. 1988 Aerodynamic focusing of particles in a carrier gas. *J. Fluid Mech.* **195**, 1–21.

Guckenheimer, J. & Holmes, P. 1983 *Nonlinear oscillations, dynamical systems and bifurcations of vector fields.* New York: Springer-Verlag.

Happel, J. & Brenner, H. 1965 Low Reynolds number hydrodynamics. Englewood Cliffs, New Jersey: Prentice Hall.

Jeffery, G. B. 1922 The motion of ellipsoidal particles immersed in a viscous fluid. *Proc. R. Soc. Lond.* A **102**, 161–179.

Levich, V. 1962 *Physico-chemical hydrodynamics.* Englewood Cliffs, New Jersey: Prentice Hall.

Lichtenberg, A. J. & Lieberman, M. A. 1983 *Regular and stochastic motion.* New York: Springer.

McLaughlin, J. B. 1988 Particle size effects on Lagrangian turbulence. *Phys. Fluids* **31**, 2544–2553.

Mallier, R. & Maxey, M. 1990 The settling of nonspherical particles in a cellular flow field. *Phys. Fluids.* (Submitted.)

Maxey, M. R. 1987*a* The motion of small spherical particles in a cellular flow field. *Phys. Fluids* **30**, 1915–1928.

Maxey, M. R. 1987*b* The gravitational settling of aerosol particles in homogeneous turbulence and random flow fields. *J. Fluid Mech.* **174**, 441–465.

Maxey, M. R. & Corrsin, S. 1986 Gravitational settling of aerosol particles in randomly oriented cellular flow fields. *J. Atmos. Sci.* **43**, 1112–1134.

Maxey, M. R. & Riley, J. J. 1983 Equation of motion for a small rigid sphere in a nonuniform flow. *Phys. Fluids* **26**, 883–889.

Ottino, J. M. 1989 *The kinematics of mixing: stretching, chaos, and transport.* Cambridge University Press.

Pruppacher, H. R. & Klett, J. D. 1978 *Microphysics of clouds and precipitation.* Dordrecht: Reidel.

Shin, H. 1990 Chaotic sedimentation of nonspherical particles in a cellular flow field. Ph.D. dissertation, Brown University, U.S.A.

Smith, L. A. & Spiegel, E. A. 1985 Pattern formation by particles settling in viscous flows. *Lect. Notes Phys.* **230**, 306.

Solomon, T. H. & Gollub, J. P. 1988 Chaotic particle transport in time-dependent Rayleigh–Bénard convection. *Phys. Rev.* A **38**, 6280–6286.

PHILOSOPHICAL TRANSACTIONS OF THE ROYAL SOCIETY A MATHEMATICAL, PHYSICAL & ENGINEERING SCIENCES

Stommel, H. 1949 Trajectories of small bodies sinking slowly through convection cells. *J. Mar. Res.* **8**, 24–29.

Taylor, G. I. 1921 Diffusion by continuous movements. *Proc. Lond. math. Soc.* **20**, 196–211.

Thomas, N. H., Auton, T. R., Sene, K. J. & Hunt, J. C. R. 1983 Entrapment and transport of bubbles by transient large eddies in multiphase turbulent shear flows. In *Proc. BHRA Int. Conf. on the Physical Modelling of Multiphase Flows*, pp. 169–184.

Thomas, N. H., Anton, T. R., Sene, K. J. & Hunt, J. C. R. 1984 Entrapment and transport of bubbles in plunging water. In *Gas transfer at water surfaces* (ed. W. Brutsaert & G. H. Jirka), p. 255. Dordrecht: Reidel.

Wang, L. P., Burton, T. D. & Stock, D. E. 1990 Chaotic dynamics of heavy particle dispersion: fractal dimension versus dispersion coefficients. *Phys. Fluids.* A **2**, 1305–1308.

PHILOSOPHICAL TRANSACTIONS OF THE ROYAL SOCIETY A MATHEMATICAL, PHYSICAL & ENGINEERING SCIENCES